



Contents lists available at ScienceDirect

Life Sciences

journal homepage: www.elsevier.com/locate/lifescie

Curcumin-primed exosomes mitigate endothelial cell dysfunction during hyperhomocysteinemia

Q1 A. Kalani, P.K. Kamat, P. Chaturvedi, S.C. Tyagi, N. Tyagi *

4 Department of Physiology and Biophysics, School of Medicine, University of Louisville, Louisville, KY 40202, USA

ARTICLE INFO

6 Article history:
7 Received 22 January 2014
8 Accepted 18 April 2014
9 Available online xxx

10 Keywords:
11 Blood–brain barrier
12 Curcumin
13 Endothelial cells
14 Exosomes
15 Homocysteine
16 Oxidative stress
17 Permeability
18 Tight junctions

ABSTRACT

Aim: Exosomes, the nano-units (<200 nm), released from diverse cell types in the extracellular body fluid, possess 19 non-immunogenic property and ability to cross the blood–brain barrier (BBB). Since exosomes carry biological 20 information from their cells of origin, we hypothesize that priming cells with potential therapeutic agents release 21 improved cellular contents through exosomes. Curcumin possesses anti-oxidative and anti-inflammatory proper- 22 ties and provides a promising treatment for cerebral diseases and therefore, the aim of the study is to establish 23 that mouse brain endothelial cells (MBECs) when primed with curcumin (7.5 μM), release an alleviated exosome 24 population that can help recover the endothelial cell (EC) layer permeability. 25

Main methods: Homocysteine is a well-known causative factor of BBB disruption; therefore, homocysteine-treated 26 ECs were used as a model of BBB disruption and curcumin-primed exosomes were utilized to check their potential 27 for mitigating EC disruption. MBECs were treated with curcumin and exosomes were isolated by using ultracentri- 28 fuge and immunoprecipitation. Expression levels of junction proteins were detected by Western blot and 29 immunocytochemistry assays. Endothelial cell permeability was analyzed with FITC-BSA leakage assay using 30 transwell permeable supports. 31

Key findings: Exosomes derived from curcumin-treated (primed) cells (CUR-EXO) alleviated oxidative stress, tight 32 junctions (ZO-1, claudin-5, occludin), adherent junction (VE-cadherin) proteins and EC layer permeability induced 33 during EC damage due to high homocysteine levels (hyperhomocysteinemia). 34

Significance: In conclusion, the study potentiates the use of CUR-EXO for cerebral diseases where drug delivery is still 35 a challenge. The results also pave the way to novel translational therapies for cerebral diseases by maintaining and 36 establishing therapeutic conservatories via primed exosomes. 37

© 2014 Published by Elsevier Inc.

Q4 Introduction

44 Exosomes are nano-vesicles (<200 nm) formed from the fusion of 45 internal vesicles of multivesicular bodies to plasma membrane. These 46 are found in extracellular fluids of the body (urine, breast milk, saliva, 47 cerebrospinal fluid, broncho–alveolar lavage) and culture conditioned 48 media. These nano-units are believed as a molecular source of cellular 49 factory and retain molecular conservatory of the cell type from where 50 they are released (Kalani et al., 2013c). Apart from their use in biomark- 51 er exploration, mounting literature suggests their use in therapy for 52 cerebral diseases, such as stroke (Xin et al., 2013). The major advantage 53 of their use over other therapeutic systems in cerebral diseases is 54 because of their ability to cross the BBB (blood–brain barrier, non- 55 immunogenicity and targeted delivery (Kalani et al., 2013c; Zhuang 56 et al., 2011); but the studies are largely lacking which provide sufficient

information for their therapeutic aspects to combat and alleviate BBB 57 disruption. 58

The blood–brain barrier (BBB) is exclusively maintained by cerebral 59 blood vessels, which are lined by specialized endothelial cells (ECs). The 60 integrity of cerebral ECs is retained by the cross talk of tight junctions 61 (TJs, zona occludens, claudins) and adherent junctions (VE-cadherin). 62 In pathological conditions, such as vascular complications and neuro- 63 logical disorders, cerebral junctions are disrupted that they affect the 64 selective barrier function of the BBB and eventually raise vascular per- 65 meability (de Vries et al., 1997; Kalani et al., 2013a). The BBB has been 66 reported to be affected significantly by homocysteine (Hcy) (Kalani 67 et al., 2013a), which is a natural inhabitant molecule formed from me- 68 thionine metabolism in the body. Being deficient in cystathionine-β 69 synthetase (CBS) enzyme activity, which is responsible for Hcy clear- 70 ance, the mammalian endothelium is the prime target of Hcy-induced 71 toxicity (Shastry et al., 2006). The outcome of earlier studies reflect 72 that subclinical elevation in Hcy levels (hyperhomocysteinemia; 73 HHcy) (from baseline of ~3 μmoles/l to ~12 μmoles/l) induces toxicity 74 resulting in considerable leakage of plasma proteins (Beard et al., 75 2011; Kamath et al., 2006; Lominadze et al., 2006). The subsequent 76 events that took place after the elevation of Hcy include: 1) activation 77

* Corresponding author at: Department of Physiology and Biophysics, 500 South Preston Street, Health Sciences Centre, A-1201, University of Louisville, Louisville, KY 40202, USA. Tel.: +1 502 852 4145; fax: +1 502 852 6239.
E-mail address: n0tyag01@louisville.edu (N. Tyagi).

of matrix metalloproteinases (MMPs), 2) disruption of membrane proteins including TJJs and other junctional proteins and, 3) functional decline in endothelial cells forming the BBB (Kumar et al., 2008; Lee et al., 2012).

Recently curcumin (diferuloylmethane; CUR) which is derived from the root of *Curcumin longa* (spice turmeric) has been used for neurological implications. Curcumin is also termed as yellow gold as it possesses anti-inflammatory, anti-lipidemic, and anti-oxidative properties, and has been recommended for the clinical trials to prevent/treat neurological diseases (Kulkarni and Dhir, 2010). The findings of the earlier studies implicating *in vivo* myeloid cells suggest that curcumin delivered by exosomes is more stable, highly concentrated in the blood, and exhibits therapeutic effect, rather than toxic effects (Sun et al., 2010). The study by Liu et al. highlighted the increase in exosome/microvesicle secretion with curcumin that attenuates lysosomal cholesterol traffic impairment in HepG2 hepatocarcinoma cells and THP-1 differentiated macrophages (Canfran-Duque et al., 2013). Although these reports suggest beneficiary effect of curcumin on exosome production and effect of curcumin-packed exosomes to surmount pathological conditions, the reports are largely lacking which establish the effect of curcumin-primed exosomes (CUR-EXO) in EC disruption and permeability. Curcumin-primed exosomes differ from curcumin packed exosomes in the respect that they are released by curcumin treated cells while curcumin packed exosomes are exosome entities encapsulated with curcumin. Therefore, we hypothesized that CUR-primed exosomes exhibit improved molecular constituents that help in the regulation of EC disruption. Mouse brain ECs were treated with Hcy to disrupt junction proteins, enhance permeability, and the therapeutic efficacy of CUR-EXO was observed for maintaining EC integrity.

Materials and methods

Cell culture

Mouse brain endothelial cell line (MBEC) was purchased from the American Type Culture Collection (ATCC, Menassas, VA, USA) and grown in DMEM supplemented with 4.5 g/l glucose, 3.7 g/l sodium bicarbonate, 4 mM glutamine, and exosome free 10% FBS (pH 7.4). The cells were maintained under an atmosphere of 5% CO₂ and 95% air in 25 cm² tissue culture flask.

Curcumin-primed exosome collection

MBECs were treated with curcumin (7.5 μM) for 72 h. Culture media were collected and centrifuged at 3000 ×g (10 min) and the supernatant was collected. The collected supernatant was further ultracentrifuged at 100,000 ×g (1 h) to concentrate exosomes (CUR-EXO) in pellet (They et al., 2006). CUR-EXO were purified using exo-specific beads (Life technology, Grand Island, NY, USA) as per supplier's protocol and either used for treatment or stored at –80 °C till further use. Similarly, culture media from untreated cells were also used to concentrate exosomes (EXO).

Treatment groups

The cells were given the following treatments: 1) Control, 2) Hcy (100 μM), and 3) Hcy + CUR-EXO (5 μg/ml). In some experiments, cells were treated with EXO (5 μg) and compared with CUR-EXO treated cells for the protein expression analysis of junction proteins. The EC proteins were extracted after 24 h of treatment as described earlier (They et al., 2006). The protein concentration of CUR-EXO and EXO was determined through the Bradford (Bio-Rad, Hercules, CA, USA) method as per manufacturer's protocol.

Western blotting

Exosome preparations were run on SDS-PAGE, electro-transferred and immunoblotted with anti-TSG101 (Abcam, Cambridge, MA, USA), anti-TJJs (claudin-5, ZO-1, occludin), and anti-VE cadherin specific antibodies (Santa Cruz, Dallas, Texas, USA). Images were recorded and data was analyzed with image lab software (Bio-Rad, Hercules, CA, USA).

Flow cytometry analysis

Flow cytometry was done as described earlier by Bhatnagar et al. (2007). Briefly, 5 μg CUR-EXO were incubated with 4 μm-diameter latex beads in PBS (50 μl) at RT for 20 min. The volume was increased to 300 μl and the beads were incubated at 4 °C overnight under gentle agitation. The reaction was stopped by incubation in 100 mM glycine (30 min). Coated beads were washed thrice and labeled with anti-CD63 PE and appropriate isotype control (Biolegend). After that, the beads were washed thrice and analyzed by flow cytometry (BD Accuri™ C6 Flow Cytometer, New Jersey, USA).

Gelatin zymography

In-gel gelatin zymography was performed as per our previous reports (Tyagi et al., 2011). Briefly, the protein samples were run on SDS-PAGE. The gel was washed thrice with 2.5% Triton-X 100, incubated for 24 h (37 °C) in activation buffer [5 mmol/l Tris HCl (pH 7.4), 0.005% (v/v) Brij-35, and 1 mmol/l CaCl₂], and stained with coomassie brilliant blue. Images were recorded and the data was analyzed with image-lab software (Bio-Rad, USA).

AChE activity in exosome vesicles

AChE activity in exosome vesicles was determined as described earlier (Savina et al., 2002; Stoorvogel et al., 2002). Briefly, 15 ml of exosomal preparation was suspended in 100 μl of PBS and incubated

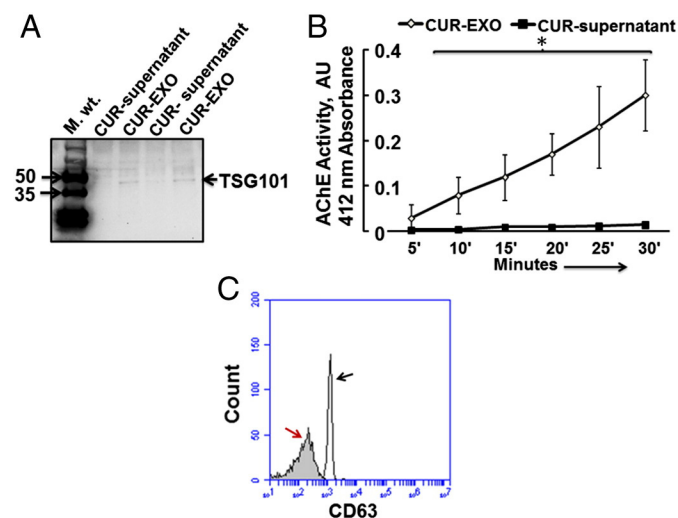


Fig. 1. Characterization of CUR-EXO: (A) Western blot analysis of CUR-EXO and CUR-supernatant fractions with anti-TSG101 antibody. (B) Line diagram for AChE activity in CUR-EXO pellet and CUR-supernatant. The OD was recorded at 419 nm at a 5 minute interval for the total time period of 30 min. Data represents mean ± SD, *p < 0.05-versus control. (C) Flow cytometry detection of CUR-EXO captured on anti-CD63 coated latex beads. The exosome-bead complexes were immunostained against CD63 (open curve, black arrow) or their corresponding isotype control (filled curves, red arrow). Data is the depiction of the three independent experiments. Here, CUR-EXO, curcumin-primed exosomes; TSG101, tumor suppressive gene 101; CUR-supernatant, supernatant collected after ultracentrifuging MBEC culture media at 100,000 ×g (devoid of CUR-EXO). (For interpretation of the references to color in this figure legend, the reader is referred to the web version of this article.)

162 with acetylthiocholine (1.25 mM) and dithio-bis-(2-nitrobenzoic acid)
 163 (0.1 mM) in a final volume of 1 ml. The incubation was carried out in cu-
 164 vettes at 37 °C and the change in absorbance (412 nm) was monitored
 165 every 5 min for the total time of 30 min.

166 Immunocytochemistry of ECs

167 Immunocytochemistry was performed to locate exosomes using
 168 PKH67 staining (Fitzner et al., 2011), determining ZO-1 cellular expres-
 169 sion, and oxidative stress using DCFH-DA (Tyagi et al., 2009). For PKH67
 170 staining, cells were grown in 8 well chamber slides and treated with tu-
 171 bulin red that binds to cytoskeleton proteins (16 h), following a PKH67
 172 labeled exosome (2 h). For ZO-1 expression, the cells were fixed with 4%
 173 paraformaldehyde (15 min), permeabilized (0.25% triton X-100 in PBS,
 174 10 min) and blocked with 1% BSA solution (30 min). Cells were further
 175 incubated with a primary antibody (overnight) and a FITC labeled
 176 secondary antibody (1 h) and washed thrice with PBS after antibody in-
 177 cubations. For DCFH-DA staining, ECs were treated with 5 μ M DCFH-DA
 178 (20 min) and washed with PBS. In the above three stainings, nuclei were
 179 stained with DAPI and cells were photographed using laser-scanning

180 confocal microscope (FluoView 1000; Olympus, PA, USA). Total fluore-
 181 scence intensity was measured with image analysis software (Image-Pro
 182 Plus; Media Cybernetics, Rockville, MD, USA).

183 EC layer permeability

184 The transwell permeable supports with polycarbonate membranes (Nu-
 185 clepore Track-Etch, 6.5 mm in diameter, 0.4 μ m pore size, and
 186 pore density of 108/cm²) coated with fibronectin were seeded with
 187 MBECs and grown in DMEM until they formed a complete monolayer
 188 (Muradashvili et al., 2012). Cells were washed with PBS and treated
 189 with 100 μ g/ml Hcy or with medium alone in the presence of FITC-
 190 BSA (0.2 mg/ml). After 6, 12, and 24 h media samples (50 μ l) were
 191 collected from lower chambers of the transwell system and the same
 192 volume of the sample was added to each appropriate upper well.
 193 Fluorescent intensity in the sample was measured by a microplate
 194 reader (SpectraMax M2e, Molecular Devices Corporation, Sunnyvale,
 195 CA, USA) with excitation at 488 nm and emission at 520 nm (cutoff
 196 515 nm). Results are expressed as a ratio of fluorescence intensity of
 197 each dye in the bottom chamber (of each experimental group) to

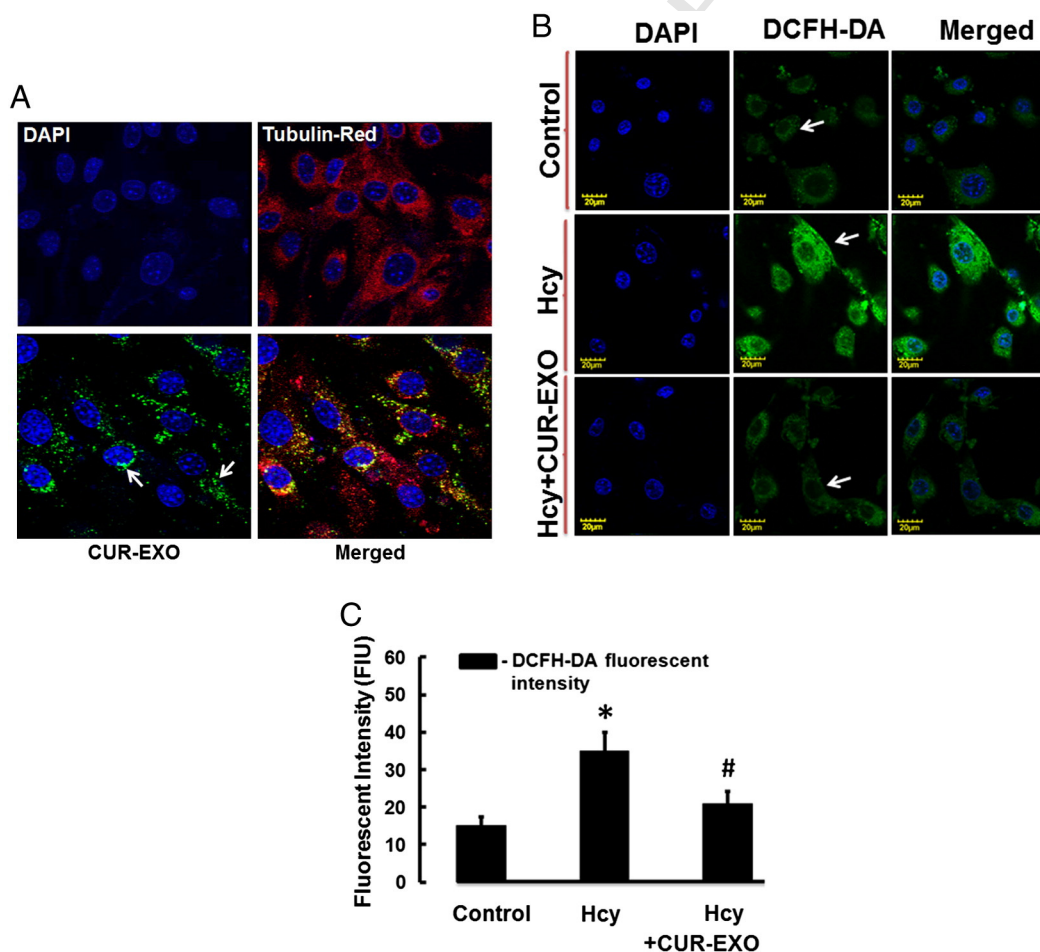


Fig. 2. CUR-EXO acquisition by the ECs and its effect on oxidative stress: (A) Confocal images showing CUR-EXO acquisition by the ECs (bottom panel). CUR-EXOs were labeled with PKH67 (green dots; indicated with white arrow), ECs were treated with tubulin red (red) and nuclei were stained with DAPI (blue). However, the green fluorescent signal was not detected in ECs undelivered with CUR-EXO (top panel). (B) Confocal images depicting oxidative stress in control, Hcy, and Hcy + CUR-EXO treated cells using DCFH-DA fluorescent dye. Green color intensity is the representation of oxidative stress as indicated by white arrows. Nuclei are stained with DAPI (blue). (C) Bar graph representing intensity of DCFH-DA dye in ECs analyzed with Image-Pro Plus 7.0 software. All Images were taken at X60 magnification, scale bar 20 μ m. Data is expressed in arbitrary units. Data represents mean \pm SD, * p < 0.05-versus control, # p < 0.05-versus Hcy-treated cells. The images and data are the representation of four independent experiments. Here, Hcy, homocysteine; CUR, curcumin; CUR-EXO-curcumin-primed exosomes; DCFH-DA, dichloro-dihydro-fluorescein diacetate (DCFH-DA); DAPI, 4',6-diamidino-2-phenylindole; ECs, endothelial cells. (For interpretation of the references to color in this figure legend, the reader is referred to the web version of this article.)

198 fluorescence intensity of the respective dye in the original sample
199 (of the respective group) at the end of the experiment.

200 *Statistical analysis*

201 The comparison between two groups was done by student's-*t* test.
202 The null hypothesis was rejected if $p < 0.05$ and considered statistically
203 significant.

Results

204

Characterization of CUR-EXO

205

To characterize CUR-EXO, Western blot, AChE activity, and flow 206
cytometry were used. Western blot analysis revealed TSG101 band in pu- 207
rified 100,000 ×g CUR-EXO pellet but not in CUR-supernatant (Fig. 1A). 208
Since exosome vesicles typically exhibit AChE activity; therefore, we 209
determined the AChE activity for CUR-EXO preparations. We got high 210

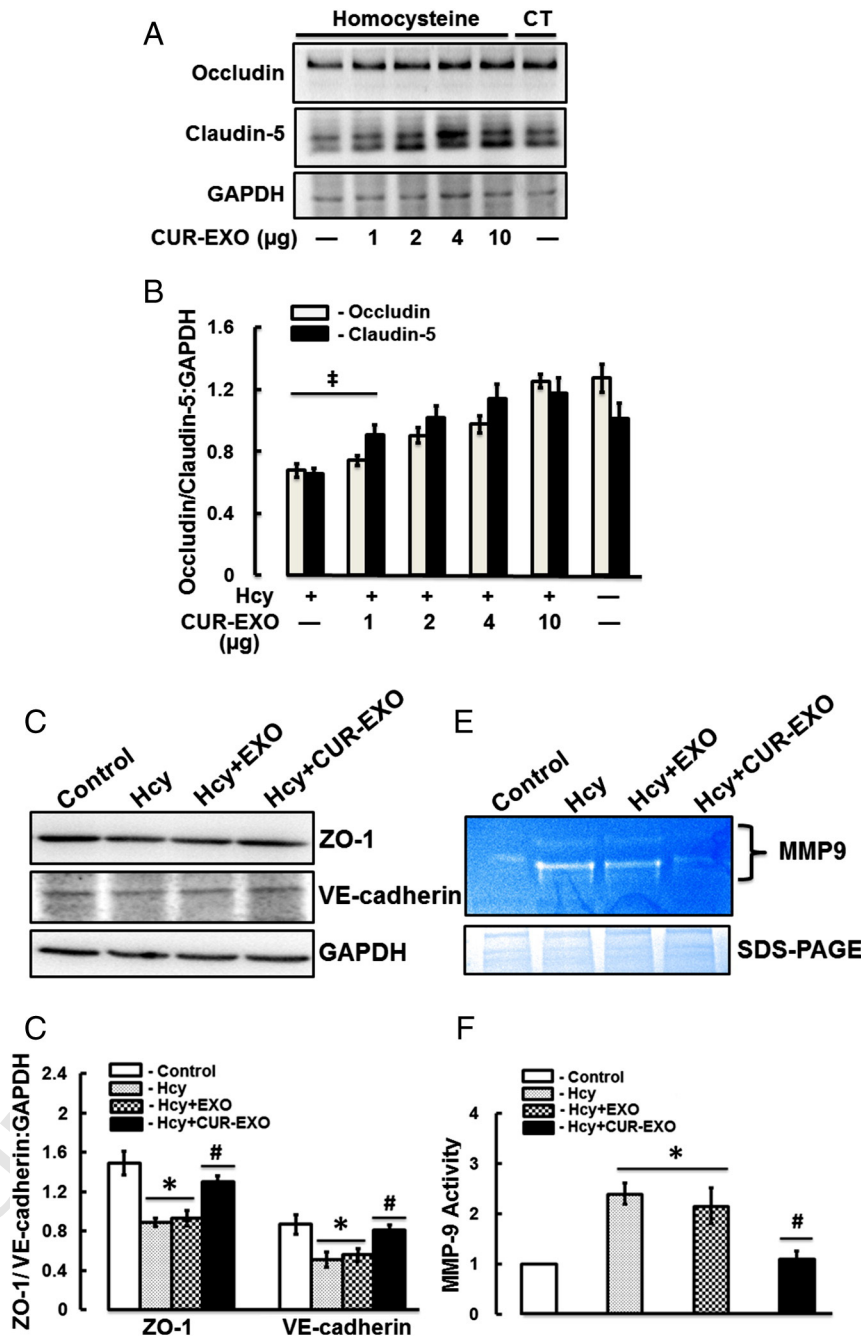
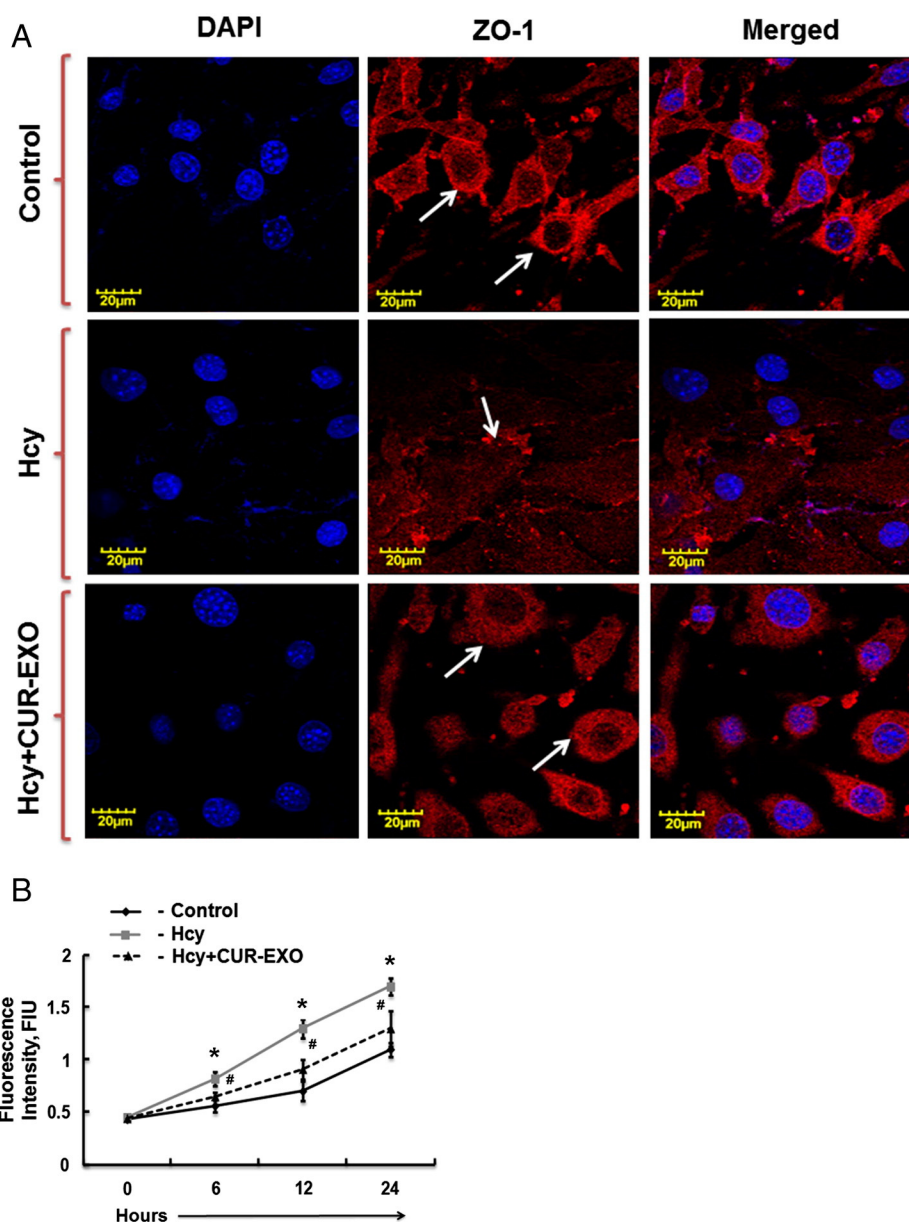


Fig. 3. Effect of CUR-EXO on junction proteins and MMP-9 gelatin degradation activity: (A) Representative Western blot images showing expression levels of occludin, claudin -5 and GAPDH in control, Hcy, and Hcy + CUR-EXO treated cells. Different concentrations (µg) of CUR-EXO were used in Hcy-treated cells. (B) Bar diagram showing densitometry analysis of occludin and claudin-5 protein expressions normalized with GAPDH. (C) Representative Western blot images showing protein expression levels of ZO-1, VE-cadherin and GAPDH in control, Hcy, Hcy + EXO, Hcy + CUR-EXO treated cells. 5 µg concentrations of EXO and CUR-EXO were used for the EC treatment. (D) Bar graph showing densitometry analysis of ZO-1 and VE-cadherin protein expressions, normalized with a GAPDH expression. (E) Representative zymograph image showing MMP-9 activity in control, Hcy, Hcy + EXO and Hcy + CUR-EXO treated cells. The EXO and CUR-EXO were used at 5 µg concentrations for treating ECs. Protein loading was shown by coomassie stained gel image given at the bottom of the gelatin zymograph image. (F) Bar graph showing densitometry analysis of MMP-9 activity. All densitometry analyses were performed through image-lab software and values are expressed as mean ± SD. # $p < 0.05$, * $p < 0.05$ -versus control, # $p < 0.05$ -versus Hcy-treated, and Hcy + EXO treated cells. Here, Hcy, homocysteine; CUR-EXO, curcumin-primed exosomes; EXO, exosomes MMP-9, matrix metalloproteinase-9.



Q2 **Fig. 4.** Effect of CUR-EXO in ZO-1 protein intensity and endothelial cell permeability: (A) Confocal images showing ZO-1 cellular expression levels (red) in control, Hcy, Hcy + CUR-EXO treated cells and indicated with white arrows. Nuclei are stained with DAPI (blue). All Images were taken at X60 magnification, scale bar 20 μ m. (B) EC layer permeability was assessed with FITC-BSA leakage in control, Hcy, Hcy + CUR-EXO treated cells using transwell permeable supports thrice at 6 h intervals for the total time period of 24 h. Data represents mean \pm SD. * $p < 0.05$ -versus control; # $p < 0.05$ -versus Hcy-treated cells. Here, Hcy, homocysteine; CUR-EXO, curcumin-primed exosomes; FITC-BSA, fluorescent isothiocyanate-bovine serum albumin; DAPI, 4',6-diamidino-2-phenylindole; ECs, endothelial cells.

211 AChE activity levels in CUR-EXO and the activity increased over the
 212 observation period of 30 min while in CUR-supernatant, devoid of
 213 exosomes, very low activity was found throughout the observation period
 214 (Fig. 1B). We further characterized CUR-EXO by using exosome-specific
 215 CD63 antibody using flow cytometry. The data showed CD63-specific
 216 peak in the flow chart as given in Fig. 1C. These results suggested the
 217 presence of CUR-EXO in purified 100,000 \times g fraction.

218 CUR-EXO acquisition by ECs and its effect on oxidative stress

219 To address the effect of CUR-EXO, we first confirmed CUR-EXO ac-
 220 quisition by ECs, by labeling CUR-EXO with PKH67 fluorescent dye. As
 221 represented in Fig. 2A, ECs incubated with labeled CUR-EXO showed
 222 green fluorescence dots as compared to control (Fig. 2A). These results
 223 suggest that CUR-EXOs are acquired by the ECs.

224 We next determined the effect of CUR-EXO on oxidative stress using
 225 DCFH-DA fluorescent dye. The confocal analysis showed an increase in
 226 oxidative stress in Hcy-treated cells as high DCFH-DA fluorescence in-
 227 tensity was found in these cells as compared to control cells (Fig. 2B).
 228 On contrary, significant reduction in oxidative stress was observed in
 229 Hcy + CUR-EXO treated cells, when compared to Hcy-treated cells
 230 (Fig. 2B, C). The decrease in oxidative stress with CUR-EXO thereby
 231 indicates its anti-oxidative properties.

232 Effect of CUR-EXO on junction proteins and MMP-9 activity

233 To address the potential of CUR-EXO to overcome Hcy-induced EC
 234 disruption, different concentrations (2, 5, 8, 10 μ g) of CUR-EXO were
 235 introduced in Hcy-treated cells and protein expressions of junction
 236 proteins (occludin, claudin-5) were determined using Western blot.

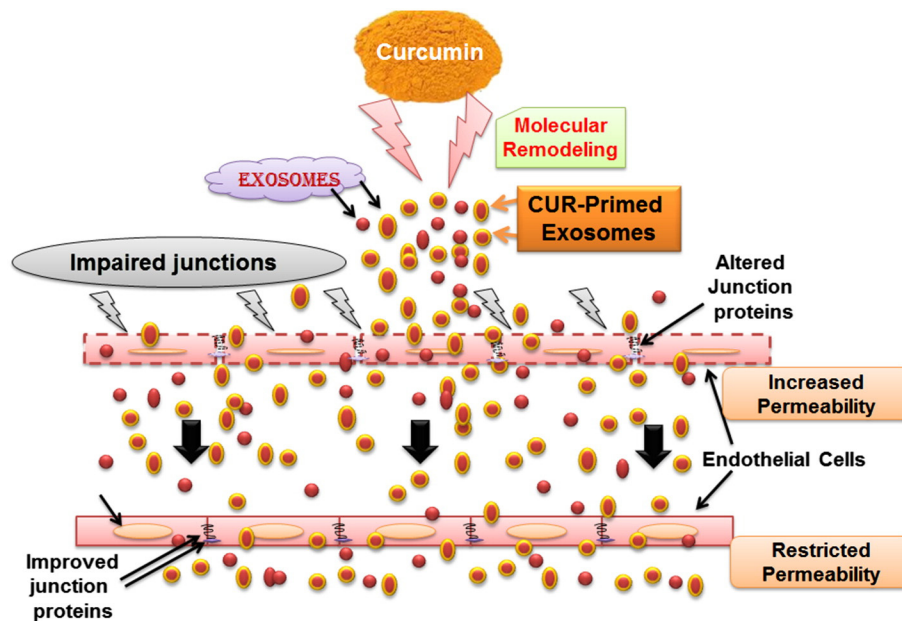


Fig. 5. Hypothesis: Overall hypothesis of the study showing the treatment of curcumin-primed exosomes recovered junction proteins, adherent junction proteins and alleviated the permeability of endothelial cells.

Significant low protein expressions of occludin and claudin-5 were observed in Hcy-treated cells as compared to control cells. On the other hand, CUR-EXO treatment alleviated the two protein levels in Hcy-treated cells (Fig. 3A, B).

In order to compare that the improvements of junction proteins are due to CUR-EXO, we compared the treatment effect of CUR-EXO with exosomes (EXO), derived from culture media of untreated cells, on the expression levels of TJs (ZO-1), and adherent junction (VE-cadherin) proteins. Western blot analysis revealed a significant loss of ZO-1 and VE-cadherins in Hcy-treated cells when compared to control cells (Fig. 3C, D). Likewise, EXO treatment to Hcy-treated cells did not show any improvement in the protein expressions of ZO-1 and VE-cadherin. On contrary, Hcy + CUR-EXO cells showed a significant improvement in the two protein expressions, as compared to Hcy-treated cells (Fig. 3C, D).

Furthermore, MMP-9 activity was determined using gelatin zymography assay. Gelatin zymography result depicted an increase in MMP-9 activity in Hcy-treated and Hcy + EXO treated cells as compared to control cells. On the other side, Hcy + CUR-EXO treated cells represented less gelatin degradation activity as comparable to Hcy-treated cells (Fig. 3E, F).

These results confirmed that CUR-EXO recovered the junction proteins and normalized the MMP-9 activity in Hcy-treated ECs to control cells.

Effect of CUR-EXO on ZO-1 expression and endothelial cell permeability

In the further sets of experiments, the effect of CUR-EXO was observed on cellular expression of ZO-1 and EC layer permeability. The confocal analysis showed very low intensity of ZO-1 in Hcy-treated cells, as compared to control cells; however, the intensity of ZO-1 was improved in Hcy + CUR-EXO treated cells (Fig. 4A).

Permeability through ECs was determined with fluorescent probe (FITC-BSA) leakage assay at different time points. Hcy-treated cells showed an increase in the leakage of FITC-BSA through ECs at all the observed time points (6, 12, 24 h) as compared to control cells. On the other side, Hcy + CUR-EXO treated cells showed a significant decrease

in leakage through ECs as compared to Hcy-treated cells (Fig. 4B). These results further confirmed the potential of CUR-EXO in the amelioration of junction proteins and EC layer permeability.

Discussion

We studied the potential of curcumin-primed exosomes on EC dysfunction by looking at their effect on junction proteins and EC permeability. Exosomes carry specific biological information (protein, nucleic acid) from the tissue type they originate. Also, they possess potentials for cerebral disease therapy and potential to be used as biomarkers. Curcumin is an anti-oxidative, anti-inflammatory and neuroprotective agent. Accumulating evidences suggest that curcumin not only induces exosome secretion but also increases its solubility, stability, and therapeutic potentials when encapsulated in exosomes (Canfran-Duque et al., 2013; Kulkarni and Dhir, 2010; Sun et al., 2010; Zhuang et al., 2011). Hence in the present study, we prepared curcumin-primed exosomes and checked their potentials against oxidative stress, TJs, and EC layer permeability.

Since the exosomes are nano-range vesicles, there have been different approaches to characterize its presence in biological fluids including culture conditioned media (Thery et al., 2006). We characterized CUR-EXO by Western blot, AChE activity and flow cytometry as described earlier (Kalani et al., 2013b; Stoorvogel et al., 2002; Thery et al., 2006). To confirm CUR-EXO acquisition by the ECs, we labeled exosomes with PKH67 fluorescent stain which specifically binds to exosomes. PKH labeling has been profoundly used to label exosomes in order to track their destinations (Fitzner et al., 2011; Zhuang et al., 2011). Increased levels of Hcy have been associated with increased permeability through ECs (Tyagi et al., 2007). Hence, we also considered Hcy-treated ECs as the model of BBB disruption. Previous studies have suggested the use of ECs as a convenient and useful model to study the BBB function (Brown et al., 2007; Watanabe et al., 2013). We earlier established that Hcy causes redox stress which induces MMP activation and increase in permeability (Tyagi et al., 2007). Therefore, in this study we checked CUR-EXO potentials to rescue these altered events.

Oxidative stress is the hallmark of pathological processes in brain ECs during HHcy (Abushik et al., 2013; Wu et al., 2013) which increases

reactive oxygen species (ROS) (Kotamraju et al., 2000), and decreases endothelial nitric oxide (NO) bioavailability (Ryter and Choi, 2002). On contrary, anti-oxidant therapy has been described to overcome the vascular remodeling and redox stress during endothelial damage (Tyagi et al., 2009). We found an increase in oxidative stress in Hcy-treated cells which was significantly decreased with CUR-EXO treatment. This suggests the anti-oxidative potential of CUR-EXO. Likewise the activity level of MMP-9, induced under HHcy, was also decreased with CUR-EXO treatment. It has also been well established that MMPs are induced in the brain ECs during Hcy-induced toxicity and lead to extracellular matrix remodeling (Kamat et al., 2013; Kumar et al., 2008; Shastry et al., 2006). The high activity of MMPs is known to disrupt the BBB by eating up junction proteins that maintain the BBB integrity (Kalani et al., 2013a; Valable et al., 2005).

Intercellular TJ protein complexes of the brain microvasculature limit the diffusion of the substances from the blood into the brain and provide cytoskeleton anchorage. ZO-1, ZO-2 and occludin are proteins linked to the actin cytoskeleton of ECs (Fanning et al., 1998; McCaffrey et al., 2009), while claudin-5 is a predominant claudin isoform, among other claudin isoforms, in TJs and its mRNA expression was found to be 600 times more as compared to other RNAs in brain ECs (Ohtsuki et al., 2008). Apart from TJs, adherent junctions are also an important regulator of the BBB permeability and attenuation of VE-cadherin, which is one of the important adherent junction proteins, showed increased monolayer permeability in culture cells, oedema and hemorrhage in *in vivo* model systems (Corada et al., 2001, 2002). These junction proteins are important to maintain selective barrier functions of ECs in brain vessels and therefore their loss affects the BBB integrity. We observed that TJs are severely down-regulated under HHcy and treatment with CUR-EXO restored TJs expressions. Additionally, the EC layer permeability that increased with Hcy treatment was improved and became comparable to control using CUR-EXO. The mechanism that we believe for CUR-EXO to rescue ECs permeability is by decreasing oxidative stress which further decreased MMP-9 in-part by alleviating TJs-adherent junctions and ECs permeability.

In conclusion, our study determined the potential use of curcumin-primed exosomes in amelioration of junction proteins and ECs permeability. The beneficiary effect of CUR-EXO is believed to be exerted by maintaining redox homeostasis, lowering MMP-9 levels, and improving TJs that eventually improve ECs permeability. Since the exosomes carry biological information from the cells of their origin, we strongly believe that the alleviations of junction proteins maintaining EC layer permeability is through the effective molecular contents in CUR-EXO imported to the cells by curcumin. Fig. 5 represents the overall hypothesis of the study.

The results of the study also direct novel future therapies by preparing improved cellular and molecular conservatories via exosomes and use them to treat cerebral diseases, for which drug penetration and access is a challenge. However, the potential limitation of the study resided to resolve the molecular signaling via CUR-primed exosome.

Conflict of interest statement

The authors declared no conflict of interest.

Acknowledgments

This work was supported by the National Institutes of Health grants HL107640-NT. The authors thank Dr. Radha Munagala for her kind suggestions in this study.

References

Abushik PA, Niittykoski M, Giniatullina R, Shakirzyanova A, Bart G, Fayuk D, et al. The role of NMDA and mGluR5 receptors in calcium mobilization and neurotoxicity of homocysteine in trigeminal and cortical neurons and glial cells. *J Neurochem* 2013.

Beard Jr RS, Reynolds JJ, Bearden SE. Hyperhomocysteinemia increases permeability of the blood–brain barrier by NMDA receptor-dependent regulation of adherens and tight junctions. *Blood* 2011;118:2007–14.

Bhatnagar S, Shinagawa K, Castellino FJ, Schorey JS. Exosomes released from macrophages infected with intracellular pathogens stimulate a proinflammatory response *in vitro* and *in vivo*. *Blood* 2007;110:3234–44.

Brown RC, Morris AP, O'Neil RG. Tight junction protein expression and barrier properties of immortalized mouse brain microvessel endothelial cells. *Brain Res* 2007;1130:17–30.

Canfran-Duque A, Pastor O, Quintana-Portillo R, Lerma M, de la Pena G, Martin-Hidalgo A, et al. Curcumin promotes exosomes/microvesicles secretion that attenuates lysosomal cholesterol traffic impairment. *Mol Nutr Food Res* 2013.

Corada M, Liao F, Lindgren M, Lampugnani MG, Breviario F, Frank R, et al. Monoclonal antibodies directed to different regions of vascular endothelial cadherin extracellular domain affect adhesion and clustering of the protein and modulate endothelial permeability. *Blood* 2001;97:1679–84.

Corada M, Zanetta L, Orsenigo F, Breviario F, Lampugnani MG, Bernasconi S, et al. A monoclonal antibody to vascular endothelial-cadherin inhibits tumor angiogenesis without side effects on endothelial permeability. *Blood* 2002;100:905–11.

de Vries HE, Kuiper J, de Boer AG, Van Berkel TJ, Breimer DD. The blood–brain barrier in neuroinflammatory diseases. *Pharmacol Rev* 1997;49:143–55.

Fanning AS, Jameson BJ, Jesaitis LA, Anderson JM. The tight junction protein ZO-1 establishes a link between the transmembrane protein occludin and the actin cytoskeleton. *J Biol Chem* 1998;273:29745–53.

Fitzner D, Schnaars M, van RD, Krishnamoorthy G, Dibaj P, Bakhti M, et al. Selective transfer of exosomes from oligodendrocytes to microglia by macropinocytosis. *J Cell Sci* 2011;124:447–58.

Kalani A, Kamat PK, Givvimani S, Brown K, Metreveli N, Tyagi SC, et al. Nutri-epigenetics ameliorates blood–brain barrier damage and neurodegeneration in hyperhomocysteinemia: role of folic acid. *J Mol Neurosci* 2013a.

Kalani A, Mohan A, Godbole MM, Bhatia E, Gupta A, Sharma RK, et al. Wilm's tumor-1 protein levels in urinary exosomes from diabetic patients with or without proteinuria. *PLoS One* 2013b;8:e61077.

Kalani A, Tyagi A, Tyagi N. Exosomes: mediators of neurodegeneration, neuroprotection and therapeutics. *Mol Neurobiol* 2013c.

Kamat PK, Kalani A, Givvimani S, Sathnur PB, Tyagi SC, et al. Hydrogen sulfide attenuates neurodegeneration and neurovascular dysfunction induced by intracerebral-administered homocysteine in mice. *Neuroscience* 2013;252:302–19.

Kamath AF, Chauhan AK, Kisucka J, Dole VS, Loscalzo J, Handy DE, et al. Elevated levels of homocysteine compromise blood–brain barrier integrity in mice. *Blood* 2006;107:591–3.

Kotamraju S, Konorev EA, Joseph J, Kalyanaraman B. Doxorubicin-induced apoptosis in endothelial cells and cardiomyocytes is ameliorated by nitric oxide spin traps and ebselen. Role of reactive oxygen and nitrogen species. *J Biol Chem* 2000;275:33585–92.

Kulkarni SK, Dhir A. An overview of curcumin in neurological disorders. *Indian J Pharm Sci* 2010;72:149–54.

Kumar M, Tyagi N, Moshal KS, Sen U, Pushpakumar SB, Vacek T, et al. GABAA receptor agonist mitigates homocysteine-induced cerebrovascular remodeling in knockout mice. *Brain Res* 2008;1221:147–53.

Lee CS, Seo YH, Yang DJ, Kim KH, Park HW, Yuk HB, et al. Positive vascular remodeling in culprit coronary lesion is associated with plaque composition: an intravascular ultrasound-virtual histology study. *Korean Circ J* 2012;42:747–52.

Lominadze D, Roberts AM, Tyagi N, Moshal KS, Tyagi SC. Homocysteine causes cerebrovascular leakage in mice. *Am J Physiol Heart Circ Physiol* 2006;290:H1206–13.

McCaffrey G, Willis CL, Staatz WD, Nametz N, Quigley CA, Hom S, et al. Occludin oligomeric assemblies at tight junctions of the blood–brain barrier are altered by hypoxia and reoxygenation stress. *J Neurochem* 2009;110:58–71.

Muradashvili N, Tyagi R, Lominadze D. A dual-tracer method for differentiating transendothelial transport from paracellular leakage *in vivo* and *in vitro*. *Front Physiol* 2012;3:166.

Ohtsuki S, Yamaguchi H, Katsukura Y, Asashima T, Terasaki T. mRNA expression levels of tight junction protein genes in mouse brain capillary endothelial cells highly purified by magnetic cell sorting. *J Neurochem* 2008;104:147–54.

Ryter SW, Choi AM. Heme oxygenase-1: molecular mechanisms of gene expression in oxygen-related stress. *Antioxid Redox Signal* 2002;4:625–32.

Savina A, Vidal M, Colombo MI. The exosome pathway in K562 cells is regulated by Rab11. *J Cell Sci* 2002;115:2505–15.

Shastry S, Tyagi N, Moshal KS, Lominadze D, Hayden MR, Tyagi SC. GABA receptors ameliorate Hcy-mediated integrin shedding and constrictive collagen remodeling in microvascular endothelial cells. *Cell Biochem Biophys* 2006;45:157–65.

Stoorvogel W, Kleijmeer MJ, Geuze HJ, Raposo G. The biogenesis and functions of exosomes. *Traffic* 2002;3:321–30.

Sun D, Zhuang X, Xiang X, Liu Y, Zhang S, Liu C, et al. A novel nanoparticle drug delivery system: the anti-inflammatory activity of curcumin is enhanced when encapsulated in exosomes. *Mol Ther* 2010;18:1606–14.

Thery C, Amigorena S, Raposo G, Clayton A. Isolation and characterization of exosomes from cell culture supernatants and biological fluids. *Curr Protoc Cell Biol* 2006. [Chapter 3: Unit].

Tyagi N, Moshal KS, Tyagi SC, Lominadze D. Gamma-aminobutyric acid A receptor mitigates homocysteine-induced endothelial cell permeability. *Endothelium* 2007;14:315–23.

Tyagi N, Moshal KS, Sen U, Vacek TP, Kumar M, Hughes Jr WM, et al. H2S protects against methionine-induced oxidative stress in brain endothelial cells. *Antioxid Redox Signal* 2009;11:25–33.

Tyagi N, Qipshidze N, Sen U, Rodriguez W, Ovechkin A, Tyagi SC. Cystathionine beta synthase gene dose dependent vascular remodeling in murine model of hyperhomocysteinemia. *Int J Physiol Pathophysiol Pharmacol* 2011;3:210–22.

- 455 Valable S, Montaner J, Bellail A, Berezowski V, Brillault J, Cecchelli R, et al. VEGF-induced 464
456 BBB permeability is associated with an MMP-9 activity increase in cerebral ischemia: 465
457 both effects decreased by Ang-1. *J Cereb Blood Flow Metab* 2005;25:1491–504. 466
- 458 Watanabe T, Dohgu S, Takata F, Nishioku T, Nakashima A, Futagami K, et al. Paracellular 467
459 barrier and tight junction protein expression in the immortalized brain endothelial 468
460 cell lines bEND.3, bEND.5 and mouse brain endothelial cell 4. *Biol Pharm Bull* 2013; 469
461 36:492–5. 470
- 462 Wu S, Gao X, Yang S, Liu L, Ge B, Yang Q. Protective effects of cariporide on endothelial 471
463 dysfunction induced by homocysteine. *Pharmacology* 2013;92:303–9.
- Xin H, Li Y, Cui Y, Yang JJ, Zhang ZG, Chopp M. Systemic administration of exosomes 464
released from mesenchymal stromal cells promote functional recovery and 465
neurovascular plasticity after stroke in rats. *J Cereb Blood Flow Metab* 2013;33: 466
1711–5. 467
- Zhuang X, Xiang X, Grizzle W, Sun D, Zhang S, Axtell RC, et al. Treatment of brain inflam- 468
matory diseases by delivering exosome encapsulated anti-inflammatory drugs from 469
the nasal region to the brain. *Mol Ther* 2011;19:1769–79. 470

UNCORRECTED PROOF